2014

Use of P3-Coded Transmission Waveforms to Generate Synthetic Aperture Radar Images

Romero, Ric A.

Use of P3-Coded Transmission Waveforms to Generate Synthetic Aperture Radar Images

David A. Garren
Department of Electrical and Computer Engineering
Naval Postgraduate School
Monterey, CA 93943
Email: dagarren@nps.edu

Phillip E. Pace
Department of Electrical and Computer Engineering
Naval Postgraduate School
Monterey, CA 93943
Email: pepace@nps.edu

Ric A. Romero
Department of Electrical and Computer Engineering
Naval Postgraduate School
Monterey, CA 93943
Email: rnromero@nps.edu

***Abstract*— This paper develops methods for using low probability of intercept (LPI) transmission waveforms in order to generate synthetic aperture radar (SAR) imagery. This analysis considers a specific transmission waveform based upon P3 codes in order to give phase shift keying (PSK) modulation. A matched correlation receiver is used to form SAR imagery corresponding to the transmitted P3-modulated waveforms. This analysis demonstrates the ability to generate SAR images based upon simulated radar measurements collected by a notional radar platform that can transmit and receive P3 waveforms. This work analyzes the resulting spotlight-mode SAR images that are generated using the P3 transmission waveforms.**

I. Introduction

The objective of this analysis is to examine the properties of SAR images formed using P3-modulated transmission waveforms. This analysis demonstrates the ability to form SAR images based upon simulated radar measurements collected by a notional radar sensor with a LPI-SAR capability. The SAR image formation quality and LPI performance corresponding to this PSK waveform is analyzed and discussed.

Giusti and Martorella [3] have used a particular type of LPI waveforms – specifically, the Frequency-Modulated Continuous Wave (FMCW) waveforms – to generate Inverse SAR (ISAR) images. The present analysis considers the use of P3-coded waveforms [9], [2], [7], which form another type of LPI waveform, in order to form SAR images of a stationary scene using spotlight-mode SAR techniques. Spotlight-mode SAR is a radar imaging mode [6], [10], [1], [5], [11] which continuously steers the radar mainbeam in the direction of a single fixed point on the ground. This SAR imaging mode can yield good image resolution, but it has a lower area coverage rate than that of stripmap SAR.

The next section defines the overall geometry and coordinates that are used in this analysis. Section III presents the details of the P3-coded transmission waveform that is assumed in generation of the SAR images. Section IV describes the methods used to compute the ideal impulse response of the target scene for each of the transmission waveforms within the synthetic aperture. Section V gives the techniques used to compute the simulated radar echoes that enter the receiver for each position along the synthetic aperture. Section VI presents the convolution method used in the correlation receiver used to generate the SAR complex I and Q channels. Section VII describes the spotlight SAR image formation process used to generate the SAR imagery based upon the output of the correlation receiver. The conclusions are presented in the final section.

II. Geometry and Coordinates

This analysis begins with the definition of the coordinates for the radar and the scene to be imaged. Define $\{x, y, z\}$ to be a spatial Cartesian coordinate system, with the $z = 0$ coordinate surface defining the target ground plane with $\{x, y, z\} = \{0, 0, 0\}$. This coordinate origin is equal to the ground reference point (GRP), or equivalently, the aim-point of the radar mainbeam for the spotlight SAR collection. The coordinate z increases with increasing elevation above the ground plane. The positive x coordinate is defined to correspond with increasing ground range from the radar. Finally, the y coordinate lies in the ground cross-range direction, so that $\{x, y, z\}$ forms a right-handed coordinate system.

Assume that the radar transmits and receives a series of radar waveforms during a total synthetic aperture time of T_0. Also, define t to be the slow-time coordinate for the mean time corresponding to the transmission and reception of a single radar waveform. Without loss in generality, define $t = 0$ to be the mid-point in time of the full synthetic aperture collection period. Thus, the slow-time t is assumed to vary between $-T_0/2$ and $T_0/2$ over the full synthetic aperture of the collection. Also, the ground down-range x coordinate lies along the projected line in the ground plane from the radar aperture center-point at $t = 0$ to the GRP. The ground cross-range coordinate y lies mutually perpendicular to the x and z coordinates.

In order to perform the required calculations, it is necessary to develop a viable parameterization of a radar platform trajectory corresponding to a straight and level flight path with constant speed and a broadside radar imaging geometry. One possible parameterization of this standard spotlight SAR imaging platform is the following in terms of a ground plane Cartesian coordinate system $\{x, y, z\}$:

$$X(t) = -X_0, \tag{1}$$

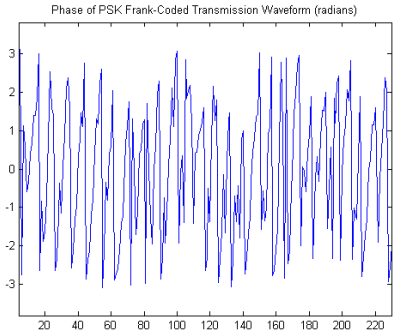

Fig. 1. Phase of the Transmitted P3-Coded Waveform

$$Y(t) = \pm V_0 t, \tag{2}$$

$$Z(t) = Z_0, \tag{3}$$

with V_0 equal to the speed of the radar platform, with X_0 equal to the radar ground range relative to the synthetic aperture center, and Z_0 equal to the radar elevation above the ground plane. Recall that the origin of the global Cartesian coordinates is selected to be the fixed aim-point on the ground to which the radar mainbeam is pointed during this spotlight SAR image collection interval. This aim-point of the radar is also referred to as the GRP. The positive sign in (2) denotes radar motion in the $+y$ direction, and the minus sign defines movement in the $-y$ direction. From (1)-(3) above, the azimuth and elevation angles, respectively, of the radar platform relative to the GRP can be defined via:

$$\theta(t) \equiv \arctan\left(\frac{Y(t)}{X(t)}\right), \tag{4}$$

$$\varphi(t) \equiv \arctan\left(\frac{Z(t)}{\sqrt{X^2(t) + Y^2(t)}}\right). \tag{5}$$

III. Transmission Radar Waveform

The P3 code is a discrete-phase code that is derived from linear frequency modulation. Specifically, the P3 code is obtained by taking the discrete phases of a linear chirp waveform via [9], [2], [7]

$$\omega_i \equiv \frac{\pi\{i-1\}^2}{N_c}, \quad \{i = 1, ..., N_c\} \tag{6}$$

with N_c equal to the pulse compression ratio. A plot of this waveform is provided in Figure 1. The reciprocal of the constant time interval between phase changes, i.e., $1/\Delta t$, is the temporal bandwidth of the waveform.

Let $q(t)$ denote the transmission waveform as a function of time t. The corresponding waveform in the spatial along-range r domain is given by

$$p(r) \equiv q(t = 2r/c), \tag{7}$$

with c denoting the speed of light and the factor of 2 arising from the round-trip propagation of the waveform. The zero position of the transmission waveform is defined so that the mean waveform energy lies at the temporal value $t = 0$, corresponding to $r = 0$ in the spatial domain.

Define the ideal complex-valued radar reflectivity to be described by the function $f(x, y, z)$ at the scene where the radar mainbeam is pointed. This function represents the ideal complex-valued impulse response of the scene, which typically contains many variations of both specular and diffuse scattering objects. In reality, the reflectivity function itself $f(x, y, z)$ can have some variation with regards to the observation angles θ and ϕ due to shadowing

IV. Idealized Radar Echoes

The idealized radar echo is defined to be the reflected radar waveform formed from the complex superposition of the multitude of scattering mechanisms within the spatial scene where the radar beam is steered, in the limit as the pulse width of the transmission waveform approaches zero. Of course, such an infinitely narrow pulse waveform uniformly excites all frequencies. Stated in another way, the idealized radar echo is the scattering response to a scene due to an infinitely sharp impulse transmission waveform.

Assume that there are some number of discrete radar scattering centers that are "visible" to the radar at a given elevation angle θ and azimuthal angle ϕ describing the instantaneous radar sensor location relative to the scene center. Assume that each scattering center in the scene can be characterized by a complex-valued reflectivity σ and a location $\{x, y, z\}$ in the physical three-dimensional space within the scene of interest.

The idealized impulse of the projection range profile has the form:

$$\tilde{g}_{\theta,\phi}(\rho) = \int dx \int dy \int dz\, f(x, y, z) \\ \delta\Big(x\cos(\theta)\cos(\phi) + y\cos(\theta)\sin(\phi) + z\sin(\theta) - s\Big). \tag{8}$$

This equation is basically a form of the 3-D Radon transform [8], [4].

In the simulation, a number of idealized point targets are inserted onto the ground plane in the approximate shape of a rectangle with a few additional points within the region. The corresponding idealized radar echo at the initial radar platform location along the synthetic aperture is shown in Figure 2

V. Received Radar Echoes

To obtain the radar waveform that enters the receiver, compute the correlation of the ideal scene response at this set of measurement aspect angles $\{\theta, \phi\}$ with the transmission waveform, i.e.,

$$g_{\theta,\phi}(s) = p(s) * \tilde{g}_{\theta,\phi}(s). \tag{9}$$

Thus, a P3-coded radar waveform is transmitted and received at each set of measurement angles $\{\theta, \phi\}$ due to different values of the idealized received radar echo from the scene at each set of $\{\theta, \phi\}$.

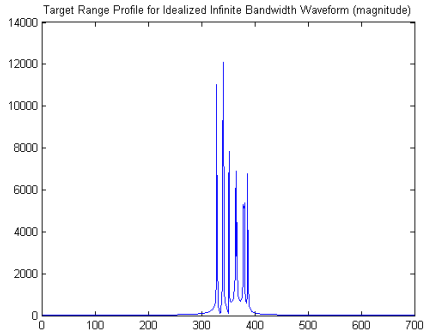

Fig. 2. Idealized radar echo at the initial radar platform location along the synthetic aperture

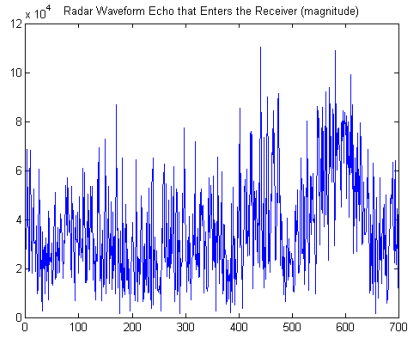

Fig. 3. Radar echo due to the simulated P3-coded waveform at the initial radar platform location along the synthetic aperture

As part of the spotlight SAR image formation process, the offset for the ideal received waveform is set so that an idealized point scattering center located at the ground reference point (GRP) $\{x, y\}$ corresponds to the value $s = 0$. For conventional SAR processing, the mean time of the transmission waveform $q(t) = p(ct/2)$, so that $s = 0$ corresponds to the mean time of the waveform $p(s)$ in the spatial domain.

For the simulation, the radar echo entering the receiver front-end, which is due to the radar reflections from the scene-of-interest is shown in Figure 3

VI. Correlation Receiver Processing

In order to model the receiver processing, the idealized radar echo for the interrogated scene at some particular set of aspect and elevation angles is convolved with the selected P3-coded radar waveform used for this particular set of measurements angles. The result of this correlation receiver processing is obtained by computing the convolution of the received waveform with the complex conjugate of the transmission waveform at the set of measurement angles under interrogation. This processing yields the range profile of the scene corresponding to each transmitted P3-coded waveform along the synthetic aperture. This correlation processing effectively dispreads the radar echoes that enter the receiver, so that range profiles are extracted from the scene consistent with the sidelobe

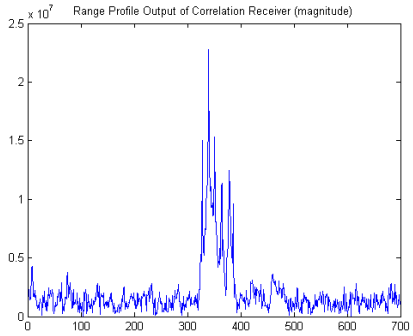

Fig. 4. Output of the correlation receiver due to the simulated P3-coded waveform at the initial radar platform location along the synthetic aperture

properties of P3 waveforms. The resulting complex-valued range profiles enable the formation of resulting SAR imagery.

The result of the ideal correlation processing is obtained by taking the convolution of the complex conjugate of the transmitted waveform with the received radar echo from the scene location where the gain of the radar transmission beam is steered for that particular waveform. For the receiver processing, the received radar echo function $g_{\theta,\phi}(s)$ is convolved with the radar waveform used for the particular set of measurements angles $\{\theta, \phi\}$. The result of this correlation receiver processing is obtained by computing the convolution of the received waveform $g^*_{\theta,\phi}(s)$ with the complex conjugate of the spatially-reflected transmission waveform at the set of measurement angles under interrogation, i.e., $p^*_{\theta,\phi}(-s)$, yielding the range profile of the scene at the set of measurement angles $\{\theta, \phi\}$, i.e.,

$$h_{\theta,\phi}(s) = p^*_{\theta,\phi}(-s) * g_{\theta,\phi}(s). \quad (10)$$

For the simulation, the output of the correlation receiver is shown in Figure 4

VII. Image Formation

The correlation receiver yields the complex I and Q channels for each transmitted waveform along the synthetic aperture. These two channels are combined to give the complex phase history data for the SAR collection. Specifically, the complex magnitude of the two channels gives the magnitude, and the $\arctan$ of the ratio of Q over I gives the phase. These data are collected at the various frequencies $f_{m'}$ covered by the radar waveforms and at the different times t along the synthetic aperture. These signal processing operations yield the down-converted, frequency-domain SAR measurement data in the original "polar" format:

$$\tilde{G}(f_{m'}, t_{n'}) = \Sigma_i \sigma_i \exp(-j2\pi \Delta R_i(t_{n'}) 2 f_{m'}/c). \quad (11)$$

In this equation, the path difference relative to the GRP is defined by

$$\Delta R_i(t_{n'}) \equiv R_i(\theta(t_{n'}), \varphi(t_{n'})) - R_0(\theta(t_{n'}), \varphi(t_{n'})). \quad (12)$$

In (11), the complex-valued measured quantities $\tilde{G}$ give both the real (i.e., in phase) and imaginary (i.e., quadrature)

components of the sub-band centered on frequency sample value $f_{m'}$ corresponding to the P3 radar waveform received at slow-time sample value $t_{n'}$. The constant c is the speed of light, and $j = \sqrt{-1}$ is the imaginary constant. The factor of 2 in the argument of the exponential function accounts for the two-way propagation of the radar. In (11), the summation over i applies to extended targets having multiple scattering centers. In (12), the quantity $R_i(\theta(t_{n'}), \varphi(t_{n'}))$ is equal to the range or distance from the radar platform for the radar waveform received at slow-time $t_{n'}$ to the ith scattering center characterized by the complex-valued reflectivity σ_i:

$$R_i(\theta(t_{n'}), \varphi(t_{n'})) = \sqrt{\{X(t_{n'}) - \alpha(t_{n'})\}^2 + \{Y(t_{n'}) - \beta(t_{n'})\}^2 + \{Z(t_{n'})\}^2} \quad (13)$$

Likewise, $R_0(\theta(t_{n'}), \varphi(t_{n'}))$ equals the range from the radar platform to the spotlight SAR GRP lying at the $\{x, y, z\} = \{0, 0, 0\}$ coordinate origin, i.e.,

$$R_0(\theta(t_{n'}), \varphi(t_{n'})) = \sqrt{\{X(t_{n'})\}^2 + \{Y(t_{n'})\}^2 + \{Z(t_{n'})\}^2}. \quad (14)$$

The waveform analysis developed herein is applied specifically to spotlight SAR image data in the ground plane of $z = 0$. In order to obtain such ground plane image data, it is convenient to define the following functions that delineate the ground range and the ground cross-range components of the spatial frequency, respectively,

$$\xi_m(f_{m'}, t_{n'}) \equiv \frac{2f_{m'}}{c} \cos(\theta(t_{n'})) \cos(\varphi(t_{n'})), \quad (15)$$

$$\eta_m(f_{m'}, t_{n'}) \equiv \frac{2f_{m'}}{c} \cos(\theta(t_{n'})) \sin(\varphi(t_{n'})). \quad (16)$$

A polar-to-rectangle sampling operation [5], or a similar procedure, must be applied to obtain the desired Cartesian-sampled data, i.e.,

$$\tilde{G}(f_{m'}, t_{n'}) \underset{\text{pol}}{\rightarrow} G(\xi_m, \eta_n). \quad (17)$$

Here, $G(\xi_m, \eta_n)$ denotes the complex-valued frequency-domain Cartesian data in terms of M discrete resampled values of the ground range spatial frequency ξ_m and N discrete resampled values of the ground cross-range spatial frequency η_n. From these data, a 2D discrete Fourier transform (DFT) yields the desired spotlight SAR image:

$$G(\xi_m, \eta_n) \underset{\text{2D DFT}}{\longleftrightarrow} b(x_k, y_\ell). \quad (18)$$

The resultant SAR image formed using P3-coded transmission waveforms is shown in Figure 5. The locations of the strong energy points within this image are consistent with the locations of the idealized point scattering centers that were inserted into the ground-plane. Thus, a successful SAR image was formed using P3-coded transmission waveforms. Figure 5 indicates that the range sidelobes (vertical) are higher than that of the cross-range direction (horizontal). These image properties follow from the correlation properties of the P3 waveform.

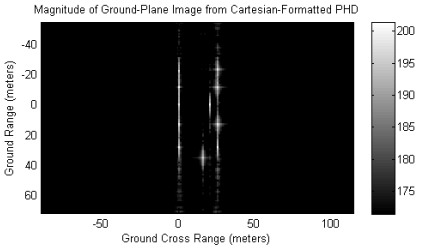

Fig. 5. The resultant SAR image formed using P3-coded transmission waveforms

VIII. Conclusions

This paper has examined methods for using P3-coded transmission waveforms for forming spotlight-mode SAR images. Simulations are developed based upon a matched correlation receiver corresponding to the transmitted P3-modulated waveforms. This analysis demonstrates the ability to form SAR images via P3-coded transmission and receiver processing.

Acknowledgment

DoD Distribution Statement A: Unlimited Distribution. The views expressed in this document are those of the authors and do not reflect the official policy or position of the Department of Defense or the U.S. Government.

References

[1] W. G. Carrara, R. S. Goodman, and R. M. Majewski, "Spotlight Synthetic Aperture Radar Signal Processing Algorithms" Artech House, Norwood, MA 1995

[2] B. W. Gillespie and L. E. Atlas, "Optimizing time-frequency kernels for classification" IEEE Transactions on Signal Processing, Vol. 49, No. 3, pp. 485-496, March 2001.

[3] E. Giusti and M Martorella, Range Doppler and Image Autofocusing for FMCW Inverse Synthetic Aperture Radar IEEE Transactions on Aerospace and Electronic Systems, Volume 47, Issue 4, October 2011, pages 2807-2823.

[4] A. K. Jain, Fundamentals of Digital Image Processing", Prentice Hall, Englewood Cliffs, NJ, 1989.

[5] C. V. Jakowatz Jr., D. E. Wahl, P. H. Eichel, D. C. Ghiglia, and P. A.Thompson, "Spotlight-Mode Synthetic Aperture Radar: A Signal Processing Approach", Kluwer Academic, Norwell, MA, 1996.

[6] D. C. Munson, Jr., J. D. O'Brien and W. K. Jenkins, "A tomographic formulation of spotlight-mode synthetic aperture radar" Proceedings of the IEEE, Vol. 71, No. 8, pp. 917-925, 1983.

[7] P. E. Pace, "Detecting and Classifying Low Probability of Intercept Radar" 2nd ed., Artech House, Boston, 2009.

[8] J. Radon, "Uber die Bestimmung von Funktionen durch ihre Integralwerte Tangs gewisser Mannigfaltikeiten (On the determination of functions from their integrals along certain manifolds)", Math. Phys. Klass, Vol. 69, pp. 262-277, 1917.

[9] C. P. Shelton, Human Interface/Human Error," em Dependable Embedded Systems, Carnegie Mellon University, pp. 18-849b Spring 1999.

[10] J. L. H. Webb and D. C. Munson, Jr., "SAR image reconstruction for an arbitrary radar path" in 1995 International Conference on Acoustics, Speech, and Signal Processing in Detroit, MI, on 09-12 May 1995.

[11] S. Xiao and D. C. Munson, Jr., "Spotlight-mode SAR imaging of a three-dimensional scence using spectral estimation techniques", Geoscience and Remote Sensing Symposium Proceedings, 1998. IGARSS '98. 1998 IEEE International, Vol. 2, pp. 642-644.